

# Thermal properties of halogen-ethane glassy crystals: Effects of orientational disorder and the role of internal molecular degrees of freedom

G. A. Vdovichenko, A. I. Krivchikov, and O. A. Korolyuk

*B. Verkin Institute for Low Temperature Physics and Engineering of NAS Ukraine, 47 Lenin Ave., 61103 Kharkov, Ukraine*

J. Ll. Tamarit,<sup>a)</sup> L. C. Pardo, and M. Rovira-Esteva

*Grup de Caracterització de Materials, Departament de Física i Enginyeria Nuclear, ETSEIB, Universitat Politècnica de Catalunya, Diagonal 647, 08028 Barcelona, Catalonia, Spain*

F.J. Bermejo

*Instituto de Estructura de la Materia, CSIC, Consejo Superior de Investigaciones Científicas, Serrano 123, 28006 Madrid, Spain*

M. Hassaine and M. A. Ramos

*Laboratorio de Bajas Temperaturas, Departamento de Física de la Materia Condensada, Condensed Matter Physics Center (IFIMAC) and Instituto Nicolás Cabrera, Universidad Autónoma de Madrid, Francisco Tomás y Valiente 7, 28049 Madrid, Spain*

The thermal conductivity, specific heat, and specific volume of the orientational glass former 1,1,2-trichloro-1,2,2-trifluoroethane ( $\text{CCl}_2\text{F} - \text{CClF}_2$ , F-113) have been measured under equilibrium pressure within the low-temperature range, showing thermodynamic anomalies at ca. 120, 72 and 20 K. The results are discussed together with those pertaining the structurally-related 1,1,2,2-tetrachloro-1,2-difluoroethane ( $\text{CCl}_2\text{F} - \text{CCl}_2\text{F}$ , F-112), which also shows anomalies at 130, 90 and 60 K. The rich phase behavior of these compounds can be accounted for by the interplay between several of their degrees of freedom. The arrest of the degrees of freedom corresponding to the internal molecular rotation, responsible for the existence of two energetically distinct isomers, and the overall molecular orientation, source of the characteristic orientational disorder of plastic phases, can explain the anomalies at higher and intermediate temperatures, respectively. The soft-potential model has been used as the framework to describe the thermal properties at low temperatures. We show that the low-temperature anomaly of the compounds corresponds to a secondary relaxation, which can be associated with the appearance of Umklapp processes, i.e. anharmonic phonon-phonon scattering, that dominate thermal transport in that temperature range.

PACS numbers: 66.70.Hk, 65.60.+a, 63.50.Lm, 64.70.P-

## I. INTRODUCTION

The term *plastic* or *rotator-phase crystal* denotes a crystalline arrangement of weakly interacting bodies, often of molecular nature, which albeit showing translational long-range order, exhibit dynamical orientational disorder, namely the bodies forming the plastic crystal maintain their overall position anchored to the lattice points, but experience thermal reorientation fluctuations.<sup>1,2</sup> The existence of these degrees of freedom has long been known to be the reason for the mechanical softness and low melting enthalpy of plastic crystals.

When cooled down below low-enough temperatures, some plastic crystals show specific heat and dynamic anomalies characteristic of glass transitions.<sup>3</sup> At the temperature where such glass transition take place, the dynamical orientational disorder of the plastic crystal becomes arrested and a quasi-static orientationally-disordered crystal is obtained. This kind of arrested crystal is known as *orientational glass* or *glassy crystal*.<sup>3,4</sup>

Additionally, other degrees of freedom, such as inter-

nal molecular rotations, can also be thermally activated within the plastic crystalline or glassy crystalline phases.

The halogen-ethane derivatives ( $\text{C}_2\text{X}_{6-n}\text{Y}_n$ , with X, Y= H, Cl, F, Br) are well known examples of compounds exhibiting this kind of solid phases. The relevance of studying such crystals stems from the fact that they are among the simplest model systems where the effects of an internal molecular degree of freedom, such as the rotation about the C – C chemical bond, can be investigated. The flexibility of this bond allows one side of the molecule to rotate with respect to the other, which leads in many compounds to two energetically distinct rotamers or conformational isomers. Although the energy barrier between the conformers, which has recently been determined within the gas phase for one of the compounds is large (i.e. of the order 5 - 6 kcal/mol depending upon the conformer, LeBris2007) of the energy difference between conformers is much smaller (about 0.38 kcal/mol LeBris2007), and is expected to significantly decrease within the condensed phases since such lowest frequency internal modes strongly couple to the lattice motions. In addition, the coexistence of two conformers has been observed in the vapor, liquid and solid states.<sup>5-11</sup>

The interplay of the many degrees of freedom within these systems hinders the nucleation of their stable

---

<sup>a)</sup>Electronic mail: josep.lluis.tamarit@upc.edu

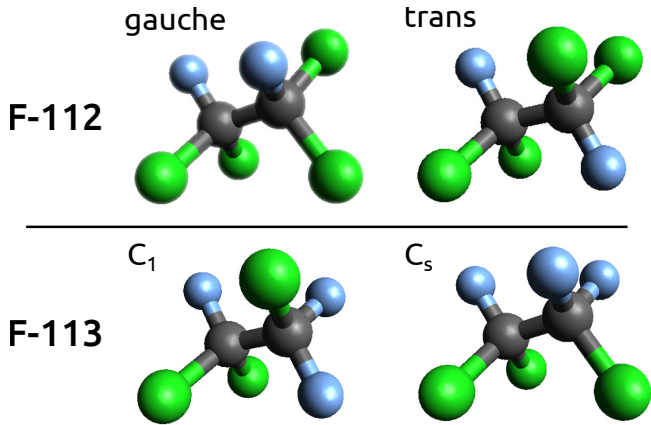


FIG. 1. Scheme of the two energetically distinct molecular rotamers of 1,1,2-tetrachloro-1,2-difluoroethane (F-112), gauche and trans, and of 1,1,2-trichloro-1,2,2-trifluoroethane (F-113),  $C_1$  and  $C_s$ . Atom codes are green for Cl, blue for F and grey for C.

phase, and thus promotes the emergence of metastable phases for a wide temperature range. Early studies by Kolesov et al. on some halogen ethanes, namely, 1,1,2,2-tetrachloro-1,2-difluoroethane ( $\text{CCl}_2\text{F} - \text{CCl}_2\text{F}$ , hereafter F-112), 1,1,2-trichloro-1,2,2-trifluoroethane ( $\text{CCl}_2\text{F} - \text{CClF}_2$ , hereafter F-113), and 1,2-dichloro-1,1,2,2-tetrafluoroethane ( $\text{CClF}_2 - \text{CClF}_2$ ), already pointed out the difficulty to obtain their low-temperature fully-ordered crystal phases.<sup>12,13</sup> In fact, the molecules of this family of compounds are so easily arrested in disordered glassy crystalline states that F-112 is the most fragile plastic crystal known so far (note that *fragility* refers here to the measure of how abruptly changes the orientational dynamics with the temperature variations).<sup>14</sup> Several authors have linked the existence of the F-112 internal molecular degree of freedom to this outstanding facility to supercool its plastic crystalline phase.<sup>14–19</sup>

Halogen-ethane derivatives have been thoroughly characterized macroscopically (heat capacity, thermodynamic magnitudes, phase transitions, etc.) and microscopically (molecular dynamics, crystallographic structure, relaxation dynamics, molecular structure, etc.) seeking to find a relation between its physical properties and its intermolecular interactions, as well as its intramolecular features, which can influence both, the short- and the long-range order.<sup>14–22</sup>

F-112 and F-113 are archetypal examples in which a mixture of conformers is present, and for which a complicated sequence of calorimetric transitions appear. The Figure 1 shows the two F-112 conformers, gauche and trans, and the two F-113 conformers,  $C_1$  and  $C_s$ .

For F-112, early specific heat ( $C_p$ ) measurements revealed three thermal anomalies namely, a step-like feature appearing about 130 K attributed to the arrest of the conformational degree of freedom, a pronounced jump in  $C_p$  at 90 K due to the orientational glass transition, and

an additional anomaly around 60 K.<sup>16</sup> Above 130 K, molecules sitting in the body-centered cubic (bcc) plastic crystal experience fluctuations in their overall orientation, as well as in their internal rotation. Below 130 K, the conformational disorder of the molecules is assumed to become frozen and they are stuck with the conformation they had at the onset of the conformational arrest, but they can still reorient as a whole and experience torsional, low-amplitude oscillations about the  $C - C$  bond. However, at  $T_g \approx 90$  K the primary glass transition takes place and the orientational disorder also becomes arrested. The anomaly at 60 K was attributed to a secondary relaxation, but it still has an unclear physical origin. While other plastic crystals exhibit no or only weak secondary relaxations, F-112's strong secondary relaxation is still a matter of controversy.

Furthermore, an unusually wide thermal conductivity plateau for F-112's glassy crystal was recently reported by some of the authors of this work. This plateau extends from 10 K up to 70 – 80 K, almost up to the glass transition temperature, and was suggested to be induced by a resonant scattering of phonons caused by simple oscillators.<sup>17</sup>

It should also be mentioned that for F-112, only a scarce 2-3 % of a more stable low-temperature crystalline phase was obtained after annealing the glassy crystalline phase for 50 days.<sup>16</sup>

In general, trans conformers are energetically favored over gauche conformers in the vapor state of most substances. However, the opposite behavior where the gauche conformer is more stable than the trans conformer, known as *gauche effect*, has been reported for a few compounds, in particular for some halogen-ethane derivatives.<sup>23–26</sup> Rovira-Esteva et al. have recently shown that this is the case for F-112 as well, and that its gauche rotational isomer is in fact more stable than the trans one, with the gauche conformer representing about 68% of the molecular population in the liquid state.<sup>15</sup>

F-113 has been much less studied. Its molecule shows two geometrical conformations related to each other by a rotation of about 120° around the CC single bond as shown in Fig. 1. One of the conformers, characterized by a *trans* position of two CCl and CF bonds, has a  $C_1$  point/group symmetry while the other one, characterized by a *gauche* position of all the CCl and CF bonds, shows  $C_s$  symmetry. Kolesov et al. measured the specific heat from 6 K up to 300 K for the various stable solid and liquid phases and reported the formation of a plastic crystalline phase below the melting temperature  $T_m = 238$  K.<sup>12,13</sup> They suggested that at the lower temperatures of the plastic crystalline phase the ratio between the  $C_1$  and  $C_s$  conformers must be frozen. This plastic crystalline phase can be easily supercooled and undergoes a glass transition into a glassy crystalline phase at  $T_g \approx 70$  K. Moreover, they were also able to obtain a more stable low-temperature crystalline phase than the glassy crystal by gradual cooling of the plastic crystal and then annealing the sample for 10 – 14 hours.

However, this low-temperature crystalline phase still has a significant amount of residual entropy, which suggests a certain degree of arrested disorder. On heating, this low-temperature crystalline phase transforms at 82.5 K into the plastic crystalline phase.

Infrared and electron diffraction studies of F-113 have shown a mixture of both  $C_1$  and  $C_s$  isomers for the plastic crystalline, liquid and vapor phases studied across the temperature range 173 – 353 K, with the  $C_1$  conformer being more stable than the  $C_s$  conformer.<sup>27–29</sup>

The purpose of the present article is to report on new measurements of the thermal properties of F-113 and to compare them to measurements of F-112, which have been already partially reported. The interest of such an exercise stems from the extremely different behavior exhibited by the thermal and transport properties of these two chemically close materials. The research reported here has focused on the effects of the thermally activated degrees of freedom of both materials on their thermal and transport properties, such as the thermal conductivity, specific heat and specific volume.

## II. EXPERIMENTAL DETAILS

We have used 1,2,2-trichloro-1,1,2-trifluoroethane ( $CCl_2F - CClF_2$ , F-113) purchased from Aldrich, with purity > 99.7 %, and 1,1,2,2-tetrachloro-1,2-difluoroethane ( $CCl_2F - CCl_2F$ , F-112) from ABCR GmbH & Co. KG, with purity > 99 %.

Structural changes across the studied temperature range were monitored using the high-intensity neutron diffractometer D1b at the Institute Laue-Langevin (ILL, Grenoble) with a wavelength of  $\lambda = 2.52$  Å. The position-sensitive detector had a step size of  $0.2^\circ$  and was set up to cover a  $2\theta$ -range from  $20^\circ$  to  $100^\circ$ .

The samples were measured through several temperature cycles with different heating and cooling rates. Slight differences were observed depending upon the thermal history, however, these differences are irrelevant for the present study. Hence, the measurements shown here correspond to a slow heating rate of 0.5 K/min within the temperature range 3 – 260 K, after previously having cooled down the sample at 1 K/min.

Specific heat measurements were carried out using a versatile calorimetric system especially designed for glass-forming liquids, and described in detail elsewhere.<sup>30</sup> In brief, the sample is enclosed in a copper cell with very thin walls, which has a resistive heating element and a carbon ceramic sensor (CCS) attached. The CCS sensor is used as thermometer and is calibrated from 1.4 K to room temperature. The cell is then inserted in a glass cryostat which either employs He or  $N_2$  liquids as cryogens, depending on the temperature range of interest. The experimental set-up includes a double chamber insert to allow an independent thermal control, and operates under a vacuum environment reaching a range of  $10^{-7} - 10^{-8}$  mbar.

Clean syringes were always employed to fill the calorimetric cell with the liquid samples, which was then immediately sealed to avoid contamination with air moisture. The mass of the F-112 sample was 0.426 g and that of the F-113 sample was 0.536 g, while the mass of the empty copper cell was 1.709 g.

Two different calorimetric methods have been employed in this work. At lower temperatures (1.7 – 20 K), we followed the thermal relaxation method, either within the standard version or within an alternative procedure devised for materials showing longer relaxation times between cell and thermal sink.<sup>30</sup> For higher temperatures (20 – 260 K), we followed a quasi-adiabatic continuous method previously implemented, which has been successfully employed in glass-forming liquids above liquid- $N_2$  temperatures and in solids above liquid-He temperatures.<sup>30–32</sup> In this quasi-adiabatic continuous method, the heat capacity is determined from a dual (cooling + heating) experiment, typically using rates around  $\pm 1$  K/min, being the differential behavior of the sample cell between both runs what provides the measurement of its heat capacity.<sup>30,32</sup> The heat capacity of the empty cell is measured in a different run to subtract the addenda contribution.

The thermal conductivity of the plastic crystalline and glassy crystalline phases of F-113 were measured under equilibrium vapor pressure in an experimental set-up that uses the steady-state potentiometric method.<sup>33,34</sup> The glassy crystalline state was prepared by cooling (above 1 K/min) of the plastic crystalline phase through the glass transition region. The thermal conductivity was measured with gradually decreasing temperature within the range 2 – 125 K, for the corresponding phase below or above  $T_g$ , following the same experimental procedure previously used in F-112, as well as in other glassy crystals and structural glasses.<sup>17,35–37</sup>

## III. RESULTS

Neutron diffraction experiments allow to determine the crystalline structures of F-113 and F-112 as a function of the temperature. Both the plastic and the glassy crystalline phases of F-113 display a bcc structure, as was also previously reported for F-112.<sup>19</sup> The Figure 2 shows the variation of the bcc lattice parameter  $a$  as a function of the temperature for both compounds. Such measurements reveal a series of signatures for F-112 at temperatures that correspond to those previously reported. Several unreported anomalies can also be observed for F-113, in these measurements even more pronounced than those of F-112.

At  $T_g \approx 72$  K the primary glass transition of the F-113 plastic crystal to a glassy crystal takes place, where the overall molecular reorientation becomes arrested. The counterpart in F-112 for such a transition occurs at about 90 K. In both cases, the glass transition is evidenced by a change in the thermal expansivity, a thermodynamic

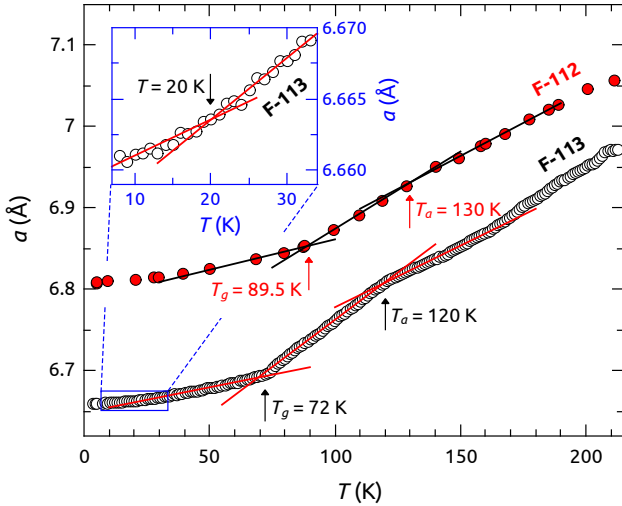


FIG. 2. (Color online) Variation of the bcc lattice parameter  $a$  as a function of temperature for F-113 (empty circles) and F-112 (full red circles). Several anomalies, qualitatively mimicking those of F-112, can be observed for F-113. Temperatures at which the different thermal anomalies discussed in the text appear, have been marked by arrows. The possible relaxational feature of F-112 at 60 K cannot be studied in these measurements for lack of data. The inset shows a magnification of the lowest temperature range for F-113 to show its behavior around the thermal feature at 20 K.

signature.

F-113 also displays a manifest variation in the thermal expansivity around 120 K. Above 120 K the molecules in the bcc lattice are able to experience overall, large/angle reorientation fluctuations, and possibly, transform from the  $C_1$  conformer into the  $C_s$ , and vice versa. Within such a view, below 120 K molecular motions are restricted to reorientation and torsional small-angle fluctuations. This hypothesis is supported by the fact that the lattice parameter features displayed by F-113 qualitatively resemble those of F-112, for which a conformational arrest was previously suggested by several authors to explain its anomaly at 130 K,<sup>15,16</sup> and is also supported by Kolesov et al.'s suggestion that the ratio between the  $C_1$  and  $C_s$  conformers is frozen at the lower temperature range of the F-113 plastic crystal.<sup>13</sup>

Finally, for F-113 the dependence of the lattice parameter with temperature also seems to change slightly at ca. 20 K. For F-112, a specific heat anomaly within the lowest temperature range, which was attributed to a secondary relaxation, was found at 60 K.<sup>16</sup> Unfortunately, this possible relaxational feature cannot be addressed in the F-112 lattice parameter measurements reported here since available data are not detailed enough for the purpose.

Additionally, the zero-temperature limits of the mass density  $\rho(0)$  of F-113 and F-112 have been obtained from the lattice parameter  $a$ , in order to determine their corresponding Debye temperatures  $\theta_D$ , which will be needed for the soft potential model (SPM) calculations. Since

there are two molecules per unit cell in the bcc lattice, the molecular volume is simply  $a^3/2$ . The zero-temperature mass density  $\rho(0)$  for the glassy crystal of each compound, can be determined by extrapolating the lattice parameter to 0 K. For F-112,  $a(0) = 6.81$  Å and hence  $\rho(0) = 2.14$  g/cm<sup>3</sup>, in good agreement with previously published values,<sup>38</sup> and for F-113,  $a(0) = 6.66$  Å and hence  $\rho(0) = 2.11$  g/cm<sup>3</sup>. The zero-mass densities  $\rho(0)$ , Debye temperatures  $\theta_D$ , and other basic thermodynamic data are summarized in Table I.

Our F-113 specific heat measurements for all temperature ranges are shown together in Figure 3. The peak corresponding to the melting transition can be found around  $T_m = 235$  K. It should be stressed the very small specific heat difference observed between the liquid and the crystalline phases at the melting temperature. Such small difference is characteristic of materials having a high degree of disorder, such as plastic crystals.

As can be seen, specific heat measurements also exhibit signatures that correlate with the anomalies found in F-113's lattice parameter. Its main glass transition (between the plastic and the glassy crystalline phases) is observed at  $T_g = 72$  K (measured at  $\sim 1$  K/min), with a discontinuity in the specific heat of  $\Delta C_p = 51.4 \pm 1.6$  J K<sup>-1</sup> mol<sup>-1</sup>. The specific heat discontinuity has been calculated by extrapolating the baselines of the glassy crystal (below  $T_g$ ) and the plastic crystal (above  $T_g$ ). Interestingly, the heat capacity curve of the glassy crystal monotonically increases with temperature, clearly surpassing the Dulong-Petit limit for a rigid molecule, which suggests a larger number of degrees of freedom being thermally activated.

The relaxational feature observed in the heat-capacity at 120 K for F-113 (see inset in Figure 3) amounts to  $\Delta C_p = 1.3 \pm 0.4$  J K<sup>-1</sup> mol<sup>-1</sup>, which is not far from that measured for F-112 at 130 K,  $\Delta C_p = 1.1 \pm 0.2$  J K<sup>-1</sup> mol<sup>-1</sup>.<sup>16</sup> Such similar values suggest that these two features could be ascribed to the same physical phenomenon for both compounds. Since the thermal anomaly in F-112 has been previously attributed to the arrest of the molecular transformations between trans and gauche conformers, this supports the idea that F-113's anomaly observed at 120 K could also arise from the arrest of the transformations between the  $C_1$  and  $C_s$  conformers.

Similar specific heat measurements conducted in F-112 (not shown here) presented a glass-like transition at  $T_g = 89.5$  K with a  $\Delta C_p = 53.8 \pm 1.5$  J mol<sup>-1</sup> K<sup>-1</sup>, which corresponds to the orientational glass transition, in very good agreement with previous data from other authors.<sup>13,16</sup>

The so-called *boson peak* can be observed in Debye-reduced specific heat  $C_p/T^3$  measurements, and is an almost universal feature of glasses,<sup>39</sup> including glassy crystals.<sup>40</sup> Figure 4 shows the reduced specific heat at low temperature for both compounds. F-113 has its boson peak maximum at  $T_{BP} = 5.0$  K, while F-112 has the maximum at  $T_{BP} = 4.5$  K.

TABLE I. Some basic thermodynamic parameters for F-112 and F-113: molecular mass ( $M$ ), orientational glass transition temperature between plastic and glassy crystalline phases ( $T_g$ ), specific heat discontinuity at  $T_g$  ( $\Delta C_p$ ), temperature of the thermal anomaly ascribed to the conformational arrest of the molecule ( $T_a$ ), temperature of the boson peak in  $C_p/T^3$  ( $T_{BP}$ ), zero-temperature mass density from neutron-diffraction data ( $\rho(0)$ ), Debye sound velocity ( $v_D$ ), and Debye temperature ( $\Theta_D$ ). The values estimated from the soft potential model fit to the specific heat  $C_p$  measurements are given in parentheses.

Glassy crystal	$M$ (g mol <sup>-1</sup> )	$T_g$ (K)	$\Delta C_p$ (J mol <sup>-1</sup> K <sup>-1</sup> )	$T_a$ (K)	$T_{BP}$ (K)	$\rho(0)$ (kg m <sup>-3</sup> )	$v_D$ (ms <sup>-1</sup> )	$\Theta_D$ (K)
F-112	203.83	89.5 <sup>a</sup> / 90 <sup>b,c</sup>	53.8 <sup>a,c</sup>	130 <sup>b</sup>	4.5 <sup>a</sup>	2140 <sup>a</sup>	1380 <sup>d</sup>	76 <sup>d</sup>
F-113	187.38	72 <sup>a</sup>	51.4 <sup>a</sup>	120 <sup>a</sup>	5.0 <sup>a</sup>	2110 <sup>a</sup>	(1420) <sup>a</sup>	(80) <sup>a</sup>

<sup>a</sup> This work.

<sup>b</sup> Ref. 17.

<sup>c</sup> Ref. 16.

<sup>d</sup> Ref. 38.

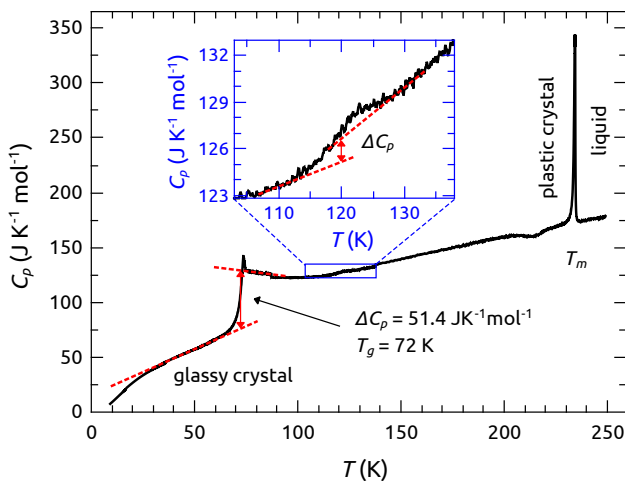


FIG. 3. (Color online) Specific heat of F-113 as a function of the temperature, where features corresponding to phase transitions and anomalies studied in this work are observed. At the higher temperature range, the melting peak indicates the transition between the liquid and plastic crystalline phases, and at 72 K the specific heat discontinuity reveals the glass transition between the plastic and glassy crystalline phases. The inset shows a magnification of the specific heat anomaly at 120 K, ascribed to the conformational arrest of the proportion between rotamers  $C_1$  and  $C_s$ .

Thermal conductivity  $\kappa(T)$  as a function of the temperature is shown in Figure 5 for the glassy and plastic crystalline phases of F-113. For the sake of comparison, previously published values are also shown for the glassy and plastic crystalline phases of F-112.<sup>17</sup> It can be seen that the thermal conductivity  $\kappa(T)$  displays for both compounds the typical behavior of glasses at low temperatures, and that of crystals at higher temperatures. More specifically, for F-113 the thermal conductivity increases with increasing temperature up to a maximum around 4.5 K. Beyond this point, a smeared plateau follows, which extends over a relatively narrow temperature range, approximately from 5 to 20 K. At about 20 K,  $\kappa(T)$  shows a kink, after which it strongly decreases with temperature until essentially the glass

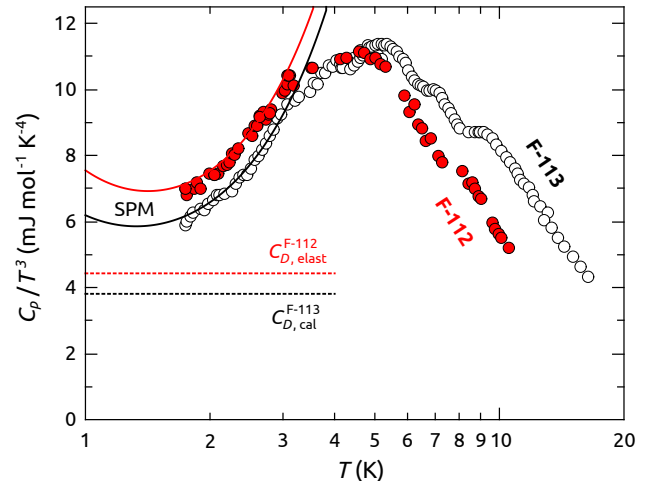


FIG. 4. (Color online) Low-temperature reduced specific heat  $C_p/T^3$  for F-112 (full red circles) and F-113 (empty circles), exhibiting the boson peak at 4.5 K and 5 K, respectively. Fits to the lower temperature range, following the soft potential model (SPM), are shown by solid lines. The Debye coefficients  $C_D$ , obtained from elasto-acoustic measurements for F-112 and from the SPM fit for F-113, are indicated by dotted lines.

transition  $T_g \approx 72$  K (corresponding to the transition between the plastic and glassy crystalline phases).

For F-112 the same qualitative behavior was previously reported.<sup>17</sup> The quantitative differences concern mainly the extension of the plateau, which persists towards the kink appearing in F-112 at about 60 K, and the significantly smaller values of  $\kappa(T)$  found at low temperatures for the glassy crystal of F-112 with respect to F-113.

On the basis of the simple phonon-gas model, the thermal conductivity is related to the phonon specific heat  $C_{ph}$ , the averaged sound velocity  $v_s$ , and the phonon mean free path  $l_{ph}$ , through the following relationship:

$$\kappa(T) = \frac{1}{3} C_{ph} v_s l_{ph}. \quad (1)$$

Taking into account the similarity of the phonon specific heat  $C_{ph}$  and the sound velocity  $v_s$  between F-112 and F-113 (see Table I), it follows that similar values

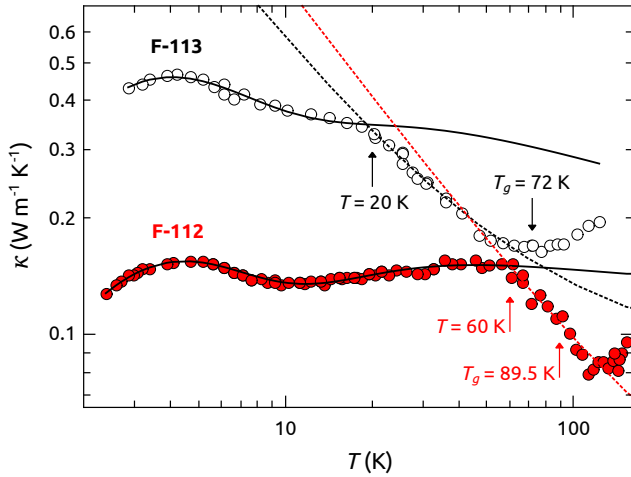


FIG. 5. (Color online) Thermal conductivity as a function of temperature (in log-log scale) for the glassy and plastic crystalline phases of F-113 (empty circles) and F-112 (full red circles). Continuous lines account for the  $\kappa_{ph}(T)$  contribution (see Equation 3). Dotted lines account for the  $\kappa(T) = A/T + B$  contribution (see Equation 7) between the low temperature anomaly and the main glass transition temperature (range from 20 K to 72 K for F-113, and from 60 K to 89.5 K for F-112).

should be expected for their low-temperature thermal conductivity. However, it can be seen in Figure 5 that this is in strong contrast with experimental results, with F-113 exhibiting much larger values than F-112. Moreover, when comparing the thermal conductivity at low temperatures for several glassy crystals (see Figure 6), it becomes clear that the unusually high values found in F-113 deserve special attention.

#### IV. DISCUSSION

At low temperatures, both specific heat and thermal conductivity of glasses or amorphous solids exhibit an astonishing universal behavior.<sup>39,43</sup> Below 1 – 2 K, the specific heat of glasses depends quasilinearly on temperature,  $C_p \propto T^{1+\delta}$ , and the thermal conductivity almost quadratically,  $\kappa \propto T^{2-\delta}$ , in contrast with the cubic dependence successfully predicted in ordered crystals for both properties by Debye’s theory.

In addition, the thermal behavior of glasses above  $\sim 2$  K and the corresponding low-frequency vibrational density of states  $g(\omega)$  around 1 THz, are dominated by another universal feature of glasses: the boson peak. This peak arises from a significant excess of the density of states  $g(\omega)$  over Debye’s prediction  $g(\omega) \propto \omega^2$ . Such “glassy excess” in low-frequency excitations translates into a broad peak in  $g(\omega)/\omega^2$ , which in turn produces a broad maximum in the reduced specific heat  $C_p/T^3$ , typically observed in glasses at 3 – 10 K.<sup>39</sup> The scattering of thermal acoustic phonons by those additional low-

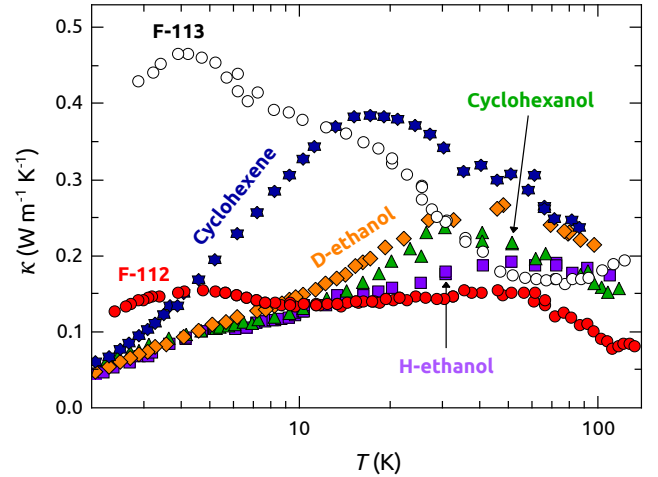


FIG. 6. (Color online) Thermal conductivity as a function of temperature (in semi-log scale) of F-113 (empty circles), and comparison of its low-temperature behavior with that of several glassy crystals previously reported: F-112<sup>17</sup> (red circles), cyclohexanol<sup>35</sup> (green triangles), H-ethanol<sup>41</sup> (violet squares), D-ethanol<sup>36</sup> (orange diamonds), and cyclohexene<sup>42</sup> (blue stars). F-113 shows remarkably high values of the thermal conductivity at low temperatures.

frequency excitations seems to be the cause of the plateau in the thermal conductivity also universally observed for any glass within that same temperature range.<sup>39,43–46</sup> Interestingly, glassy crystals have been found to exhibit the very same universal glassy behavior as truly amorphous solids.<sup>17,40,47</sup>

Thermal and acoustic properties of amorphous solids below 1 – 2 K were soon successfully accounted for by the tunneling model, which postulates a random distribution of independent tunneling states or two-level systems (TLS) from asymmetric energy barriers produced by atomic disorder.<sup>39</sup> However, thermal properties of glasses above 1 K and the corresponding low-frequency vibrational spectrum featuring the boson peak, are still much more controversial.

The soft potential model (SPM) has been used to explain the behavior at low temperatures of the two compounds. This phenomenological model can be regarded as an extension of the tunneling model and postulates the coexistence in glasses of acoustic phonons with quasilo-calized low-frequency soft modes<sup>44–46,48</sup> (for a review of the original model, see Ref. 48). Such low-frequency modes are described by a random distribution of quartic potentials, either single-well (quasiharmonic vibrations) or double-well (anharmonic two-level system) potentials. The central potential-energy parameter  $W$  of the SPM marks indeed the crossover from the region dominated by the two-level systems at the lowest temperatures, to another region where the dominant excitations are quasiharmonic soft modes. These constitute the lower frequency tail of the boson peak and the thermal conductivity plateau. The density of vibrational states in this

region dominated by soft modes is  $g(\omega) \propto \omega^4$  in the lower frequency limit.<sup>45,46</sup>

Although we have measured the specific heat and the thermal conductivity above 1.7 K and 2 K, respectively, and hence a very accurate determination of the SPM parameters is not guaranteed, we will however try to fit  $C_p$  and  $\kappa$  measurements to the SPM equations at the lowest available temperatures, in order to assess the observed low-temperature glassy excitations and the acoustic phonon contribution, as well as validating the consistency of the SPM model.

In its simplest version, the SPM coincides with the tunneling model below 1 – 2 K, predicting a quasilinear temperature dependence  $C_{\text{TLS}} T$  in the specific heat  $C_p$ , and a quadratic term in the thermal conductivity  $\kappa(T)$ . For temperatures roughly above  $W/(2k_B)$ , the specific heat is dominated by the  $C_{\text{sm}} T^5$  term arising from the soft modes, apart from the standard Debye contribution  $C_D T^3$ , and the thermal conductivity becomes roughly constant (the plateau range).<sup>45,46</sup>

Therefore, this model conveniently allows to describe the specific heat of glasses below the boson peak maximum in  $C_p/T^3$  (including glassy crystals)<sup>49</sup> through a simple equation with three contributions:<sup>49</sup>

$$C_p = C_{\text{TLS}} T + C_D T^3 + C_{\text{sm}} T^5. \quad (2)$$

In the case of F-112, previously reported values for its longitudinal sound velocity down to low temperatures, together with measurements of the elastic-stiffness coefficients below room temperature, allow to determine its Debye contribution coefficient  $C_D$ .<sup>38,50</sup> The generalized Cauchy equation  $v_L^2(T) = A + 3v_T^2(T)$ , which links longitudinal  $v_L$  and transverse  $v_T$  sound velocities, allows to determine the Debye-averaged sound velocity  $v_D$  in the zero-temperature limit.<sup>50</sup> Since the Debye contribution  $C_D T^3$  is calculated in the low-temperature limit from elasto-acoustic measurements for F-112, this means that only two parameters are needed for the SPM fit at low temperature:  $C_{\text{TLS}}$  and  $C_{\text{sm}}$ .<sup>37</sup> The  $C_D$  coefficient is determined first and, then, the two free parameters  $C_{\text{TLS}}$  and  $C_{\text{sm}}$  are obtained by a straight-linear fit well below the boson peak of  $(C_p - C_D T^3)/T$  versus  $T^4$ , as done by Hassaine et al.<sup>37</sup>

To the best of our knowledge, there are no sound-velocity values reported for the glassy crystal in the case of F-113, hence, the Debye coefficient  $C_D$  cannot be determined from elasto-acoustic measurements and all three heat capacity coefficients must be determined from the fit. Thus, we have estimated  $C_D$  and hence  $v_D$  calorimetrically from a fit of the lower temperature of the specific heat  $C_p$  measurements using the SPM model. A parabolic fit of  $C_p/T$  versus  $T^2$  at low temperatures provides the three calorimetric coefficients for the basic SPM equation, including the Debye coefficient  $C_D$ .<sup>49</sup> The SPM fits, together with the Debye contributions of F-112 and F-113 ( $C_{D, \text{elast}}^{\text{F112}}$  and  $C_{D, \text{cal}}^{\text{F113}}$ , respectively), are shown in Figure 4.

The central potential-energy parameter  $W$  of the SPM can be determined directly from the relationship  $W/k_B \approx 1.8 T_{\text{min}}$ , where  $T_{\text{min}} = (C_{\text{TLS}}/C_{\text{sm}})^{1/4}$ . Within the SPM,  $C_{\text{TLS}}$  and  $C_{\text{sm}}$  are interrelated because both are directly proportional to the density of quasilocalized soft modes. All these values are given in Table II.

On the other hand, the thermal conductivity has been studied within the framework of the SPM, employing the standard expression for the density of states of sound modes obtained in the Debye approximation:<sup>44–46,51</sup>

$$\kappa_{ph}(T) = \frac{k_B^4 T^3}{2\pi^2 \hbar^3 v_s} \int_0^{\Theta_D/T} \tau_R(x) \frac{x^4 e^x}{(1 - e^x)^2} dx \quad (3)$$

where  $x = \hbar\omega/k_B T$ ,  $v_s$  is the speed of sound averaged over longitudinal and transverse polarizations,  $\Theta_D$  is the Debye temperature, and  $\tau_R^{-1}(\omega)$  is the averaged phonon relaxation rate directly associated to the phonon mean free path.

In the SPM, the relaxation rate  $\tau_R^{-1}(x)$  is driven by three different contributions which are, the resonant scattering of sound waves by tunneling ( $\tau_{\text{TLS}}^{-1}$ ) or soft quasilocalized vibrations ( $\tau_{\text{vibr}}^{-1}$ ), and the classical relaxational processes in the asymmetric double-well potentials ( $\tau_{\text{class}}^{-1}$ ). According to the Matthiessen rule:

$$\tau_R^{-1}(\omega) = \tau_{\text{TLS}}^{-1} + \tau_{\text{vibr}}^{-1} + \tau_{\text{class}}^{-1} \quad (4)$$

If the three contributions to the SPM relaxation rate are written explicitly, we obtain the following expression<sup>44–46</sup>

$$\tau_R^{-1} = \bar{C} \pi \omega \tanh\left(\frac{\hbar\omega}{2k_B T}\right) + \ln^{-1/4}\left(\frac{1}{\omega\tau_0}\right) \bar{C} \pi \omega \left(\frac{k_B T}{W}\right)^{3/4} + \frac{\bar{C} \pi \omega}{8} \left(\frac{\hbar\omega}{W}\right)^3 \quad (5)$$

The relevant parameters in this equation are thus  $\bar{C}$ , a dimensionless constant accounting for the coupling strength between a sound wave and the soft quasilocalized mode,  $W$ , the characteristic energy of the quartic term entering the potential of the SPM, and an attempt frequency of the order of  $10^{-13}$  s.  $W$  scales the elementary excitations in the quasiharmonic soft potential in such a way that it characterizes the crossover between two regimes: one dominated by phonon scattering by two-level systems, when  $\hbar\omega \ll W$ , and another for which quasilocalized low-energy vibrational modes emerge as the main resonant scattering centers for sound waves, when  $\hbar\omega \geq W$ . It should be noted that in Equation 5 only  $\bar{C}$  and  $W$  are relevant fitting parameters, because the logarithmic factor is approximately a constant:  $\ln^{-1/4}(1/\omega\tau_0) \approx 0.7$ .

The phonon relaxation rate from Equation 5 can be used in Equation 3 to perform the fit. The parameters obtained from the SPM fit to experimental data for F-113 and F-112 are gathered in Table II, both for specific heat and thermal conductivity measurements at low temperatures. It must be emphasized that a consistent common

TABLE II. Parameters of the soft potential model obtained from the fits to specific heat and thermal conductivity measurements. The  $C_D$  value for F-112 (in parentheses) has been determined from elasto-acoustic measurements.

Glassy crystal	$W/k_B$ (K)	$\bar{C}$ ( $\times 10^{-4}$ )	$C_{\text{TLS}}$ ( $\text{mJ mol}^{-1} \text{K}^{-2}$ )	$C_D$ ( $\text{mJ mol}^{-1} \text{K}^{-4}$ )	$C_{\text{sm}}$ ( $\text{mJ mol}^{-1} \text{K}^{-6}$ )
F-112	2.5	2.8	2.50	(4.43)	0.621
F-113	2.4	0.84	1.80	3.81	0.581

$W$  value was obtained from both  $C_p$  and  $\kappa$  fits. It is also worth mentioning the close similarity of the values obtained for the  $W$  for both glassy crystals. This potential energy accounts for the crossover between the regime in which phonon scattering is due to tunneling two-level systems and that in which it is governed by quasilocalized low-frequency vibrations. Hence, according to the SPM, the temperature at which the plateau starts is quite similar for both compounds, which can be observed in Figure 5. Nevertheless, when comparing the coupling parameter  $\bar{C}$  for both glassy crystals, their behavior is quite disparate. This experimental fact evidences that for temperatures below the plateau, the scattering from low-energy excitations is much weaker for F-113 than for F-112. Even more, when comparing these  $\bar{C}$  values to those previously obtained in glassy crystals such as cyclohexanol ( $4.6 \times 10^{-4}$ ), cyanocyclohexane ( $4.8 \times 10^{-4}$ ), or ethanol ( $8.8 \times 10^{-4}$  for its glassy crystal), it is unquestioned that the  $\bar{C}$  value for F-113 clearly appears as the lowest one. The same conclusion can be achieved when compared with some structural glasses such as 2-propanol ( $5.4 \times 10^{-4}$ ), 1-propanol ( $3.1 \times 10^{-4}$ ) or ethanol ( $8.8 \times 10^{-4}$  for its structural glass).<sup>17,35</sup>

To account for a better description of the thermal conductivity at temperatures higher than  $k_B T > W$ , we will consider an additional phonon-scattering process which becomes thermally activated at those temperatures, corresponding to resonant scattering of phonons by single oscillators. Such additional contribution was already suggested for F-112 and is described by:<sup>17</sup>

$$\tau_{\text{res}}^{-1}(\omega, T) = \frac{F\omega^2 T^n}{\left[1 - \frac{\omega^2}{\omega_0^2}\right]^2 + \gamma \left[\frac{\omega}{\omega_0}\right]^4} \quad (6)$$

where  $\omega_0$  is the oscillators' average frequency.

The solid lines in Figure 5 show the thermal conductivity fits using Equation 3 with a relaxation rate  $\tau_R^{-1}(x)$  that takes into account the contributions mentioned in Equation 4 and the additional relaxation term for resonant scattering of phonons given by Equation 6. It can be seen that combining the SPM terms and the latter contribution to the phonon relaxation rate, one is able to fully account for the thermal conductivity curves from the lowest temperatures up to the wide plateau. The Table III displays the values obtained from the fit for these resonant-scattering contributions, and it evidences that they are much larger for F-112 than for F-113, as the extension of the plateau is larger for the former than for the latter. Thermal conductivity for both F-112 and F-

TABLE III. Fit parameters for F-112 and F-113 of the resonant scattering contribution by single oscillators, corresponding to Equation 6. F-113 values are from this work, and F-112 values are from Ref. 17.

Glassy crystal	$\hbar\omega/k_B$ (K)	$\gamma$	$F$ ( $s \text{K}^{-2}$ )	n
F-112	25	0.001	$5.5 \cdot 10^{-17}$	2
F-113	15	0.001	$1.2 \cdot 10^{-17}$	2

113 experiences pronounced changes at 60 K and 20 K, respectively.

However, above these temperatures, this resonant scattering mechanism is no longer dominant. Hence, to account for  $\kappa(T)$  up to the main glass transition temperatures, we resort to the fact that the materials under scrutiny are in fact translationally-ordered solids. In the high temperature region, when both the diffusive and hopping mechanisms are operative, glassy crystals can also experience the effect of the phonon-phonon scattering, which is typical of orientationally-ordered crystals above the temperature where the maximum in the phonon thermal conductivity arises. In general, the thermal conductivity of a dielectric crystal can be written as the sum of two contributions:<sup>52</sup>  $\kappa(T) = \kappa_1(T) + \kappa_2(T)$ , one due to phonons propagating with a mean-free path larger than the phonon half-wavelength, and the other attributed to localized or diffusive short-wavelength vibrational modes. Within this framework, the thermal conductivity can be approximated to a good accuracy by the expression

$$\kappa(T) = \frac{A}{T} + B \quad (7)$$

where the term  $A/T$  comprises the three-phonon Umklapp processes and the term  $B$  accounts for the additional mechanism of heat transfer that operates within the high-temperature region. Currently there is no established theory incorporating both heat transfer mechanisms. However, it is found empirically that, at sufficiently high temperatures,  $B$  can be taken as constant.<sup>53</sup> Table IV shows the parameter values resulting from using Equation 7 to fit the thermal conductivity measurements, together with the temperature ranges that have been used. It can be seen that Equation 7 satisfactorily describes the thermal conductivity in the corresponding temperature range. Such a clear  $T^{-1}$  dependence shows that the Umklapp process, which is essentially anhar-

TABLE IV. Fit parameters for the higher temperature range of the thermal conductivity, corresponding to Equation 7.

Glassy crystal	T (K)	A ( $\text{W m}^{-1}$ )	B ( $\text{W m}^{-1}\text{K}^{-1}$ )
F-112	60-90	7.8	0.02
F-113	20-70	5.0	0.085

monic phonon-phonon scattering, is dominant in that temperature range.

As far as the values are concerned, the  $A$  parameter for F-113 is slightly smaller than for F-112, which would suggest an increase of phonon scattering due to an increase of some disorder in that temperature range. On the other hand, it can be noticed that the additional terms  $B$  are smaller than the values found for orientationally-ordered molecular crystals.<sup>35,54,55</sup>

## V. SUMMARY AND CONCLUSIONS

We have measured the specific volume, thermal conductivity and specific heat of the glassy crystals of 1,2,2-trichloro-1,1,2-trifluoroethane ( $\text{CCl}_2\text{F} - \text{CClF}_2$ , F-113) and 1,1,2,2-tetrachloro-1,2-difluoroethane ( $\text{CCl}_2\text{F} - \text{CCl}_2\text{F}$ , F-112) from 1.7 K up to their plastic crystal phases, and well above the corresponding glass transition temperatures. Measurements of these crystals display a rich behavior. In this work we have focused on the discussion of the F-113 features at 20, 72, and 120 K. Several anomalies have been rationalized in terms of degrees of freedom that become arrested, such as the internal molecular rotation, which undergoes a conformational arrest ( $T_a = 120$  K), and the overall molecular rotation, which freezes at the main glass transition ( $T_g = 72$  K for F-113). These features have been compared to those of F-112, which has their counterparts at 60, 89.5, and 130 K, respectively.

The specific heat and the thermal conductivity at the lowest temperatures can be both understood by recourse to the soft potential model (SPM) which needs to be supplemented with an additional phonon-scattering contribution, ascribed to resonant scattering of phonons by single oscillators.

In stark contrast to structural glasses and other glassy crystals, the plateau exhibited by the thermal conductivity is followed by a kink and a further *decrease* in conductivity with increasing temperature up to the temperatures signaling a glass-transition. Such behavior is here attributed to a high density of thermally activated degrees of freedom due to the interplay of orientational and internal molecular low-energy motions.

The study here reported on materials exhibiting internal molecular rotational isomerism comes into line with previous studies on the structural and thermodynamic properties of materials composed by chemical isomers which have shown how a minor chemical modification can lead to strikingly disparate behaviors.<sup>56-59</sup> The results

thus call for a re-examination of some current assumptions pertaining the universality of properties exhibited by disordered matter.

## ACKNOWLEDGMENTS

This work was financially supported in part by the Spanish Ministry of Science and Innovation (grants FIS2014-54734-P, FIS2011-23488 and MAT2014-57866-REDT), by the Catalan Government (grant 2014SGR-0581) and by the Comunidad de Madrid through program NANOFRONTMAG-CM (S2013/MIT-2850), as well as by the joint NAS Ukraine and Russian Foundation for Basic Research project "Metastable states of simple condensed systems" (Agreement N 7/-2013).

<sup>1</sup>J. Timmermans, J. Phys. Chem. Solids **18**, 1 (1961).

<sup>2</sup>J. N. Sherwood, ed., *The Plastically Crystalline State (Orientationally Disordered Crystals)* (John Wiley & Sons, New York, 1978).

<sup>3</sup>H. Suga and S. Seki, J. Non-Cryst. Solids **16**, 171 (1974).

<sup>4</sup>R. W. Cahn, Nature **253**, 310 (1975).

<sup>5</sup>E. K. Plyler, J. Chem. Phys. **17**, 218 (1949).

<sup>6</sup>R. E. Kagarise and D. H. Rank, Trans. Faraday Soc. **48**, 394 (1952).

<sup>7</sup>K. Naito, I. Nakagawa, K. Kuratani, I. Ichishima, and S. Mizushima, J. Chem. Phys. **23**, 1907 (1955).

<sup>8</sup>J. P. Zietlow, F. F. Cleveland, and A. G. Meister, J. Chem. Phys. **24**, 142 (1956).

<sup>9</sup>R. E. Kagarise, J. Chem. Phys. **24**, 300 (1956).

<sup>10</sup>M. Takeda and H. S. Gutowsky, J. Chem. Phys. **26**, 577 (1957).

<sup>11</sup>J. W. Brasch, J. Chem. Phys. **43**, 3473 (1965).

<sup>12</sup>V. P. Kolesov, E. A. Kosarukina, D. Yu. Zhogin, M. E. Poloznikova, and Yu. A. Pentin, J. Chem. Thermodyn. **13**, 115 (1981).

<sup>13</sup>V. Kolesov, Thermochim. Acta **266**, 129 (1995).

<sup>14</sup>L. C. Pardo, P. Lunkenheimer, and A. Loidl, J. Chem. Phys. **124**, 124911 (2006).

<sup>15</sup>M. Rovira-Esteva, N. A. Murugan, L. C. Pardo, S. Busch, J. Ll. Tamarit, Sz. Pothoczki, G. J. Cuello, and F. J. Bermejo, Phys. Rev. B **84**, 064202 (2011).

<sup>16</sup>K. Kishimoto, H. Suga, and S. Seki, Bull. Chem. Soc. Jpn. **51**, 1691 (1978).

<sup>17</sup>I. V. Sharapova, A. I. Krivchikov, O. A. Korolyuk, A. Jezowski, M. Rovira-Esteva, J. Ll. Tamarit, L. C. Pardo, M. D. Ruiz-Martin, and F. J. Bermejo, Phys. Rev. B **81**, 094205 (2010).

<sup>18</sup>L. C. Pardo, F. J. Bermejo, J. Ll. Tamarit, G. J. Cuello, P. Lunkenheimer, and A. Loidl, J. Non-Cryst. Solids **353**, 999 (2007).

<sup>19</sup>M. Rovira-Esteva, L. C. Pardo, J. Ll. Tamarit, and F. J. Bermejo, in *Metastable Systems under Pressure*, NATO Science for peace and Security Series: A. Chemistry and Biology, edited by S. J. Rzoska, A. Drozd-Rzoska, and V. Mazur (Springer Netherlands, 2009) pp. 63-77.

<sup>20</sup>Ph. Negrier, M. Barrio, J. Ll. Tamarit, L. C. Pardo, and D. Mondieig, Cryst. Growth Des. **12**, 1513 (2012).

<sup>21</sup>Ph. Negrier, J. Ll. Tamarit, M. Barrio, and D. Mondieig, Cryst. Growth Des. **13**, 782 (2013).

<sup>22</sup>Ph. Negrier, M. Barrio, J. Ll. Tamarit, D. Mondieig, M. J. Zuriaga, and S. C. Perez, Cryst. Growth Des. **13**, 2143 (2013).

<sup>23</sup>S. Wolfe, Acc. Chem. Res. **5**, 102 (1972).

<sup>24</sup>R. C. Bingham, J. Am. Chem. Soc. **98**, 535 (1976).

<sup>25</sup>R. J. Abraham and K. Parry, J. Chem. Soc. B, 539 (1970).

<sup>26</sup>J. R. Durig, J. Liu, T. S. Little, and V. F. Kalasinsky, J. Phys. Chem. **96**, 8224 (1992).

<sup>27</sup>M. Iwasaki, Bull. Chem. Soc. Jpn. **32**, 205 (1959).

- <sup>28</sup>H. Hallam and T. Ray, *J. Mol. Spectrosc.* **12**, 69 (1964).
- <sup>29</sup>H.-N. Lee, L.-C. Chang, and T.-M. Su, *Chem. Phys. Lett.* **507**, 63 (2011).
- <sup>30</sup>E. Pérez-Enciso and M. A. Ramos, *Thermochim. Acta* **461**, 50 (2007).
- <sup>31</sup>M. Hassaine, R. J. Jiménez-Riobóo, I. V. Sharapova, O. A. Korolyuk, A. I. Krivchikov, and M. A. Ramos, *J. Chem. Phys.* **131**, 174508 (2009).
- <sup>32</sup>T. Pérez-Castañeda, J. Azpeitia, J. Hanko, A. Fente, H. Suderow, and M. A. Ramos, *J. Low Temp. Phys.* **173**, 4 (2013).
- <sup>33</sup>A. I. Krivchikov, V. G. Manzhelii, O. A. Korolyuk, B. Ya. Gorodilov, and O. O. Romantsova, *Phys. Chem. Chem. Phys.* **7**, 728 (2005).
- <sup>34</sup>A. I. Krivchikov, B. Ya. Gorodilov, and O. A. Korolyuk, *Instrum. Exp. Tech.* **48**, 417 (2005).
- <sup>35</sup>A. I. Krivchikov, O. A. Korolyuk, I. V. Sharapova, J. Ll. Tamarit, F. J. Bermejo, L. C. Pardo, M. Rovira-Esteva, M. D. Ruiz-Martin, A. Jezowski, J. Baran, and N. A. Davydova, *Phys. Rev. B* **85**, 014206 (2012).
- <sup>36</sup>A. I. Krivchikov, M. Hassaine, I. V. Sharapova, O. A. Korolyuk, R. J. Jiménez-Riobóo, and M. A. Ramos, *J. Non-Cryst. Solids* **357**, 524 (2011).
- <sup>37</sup>M. Hassaine, M. A. Ramos, A. I. Krivchikov, I. V. Sharapova, O. A. Korolyuk, and R. J. Jiménez-Riobóo, *Phys. Rev. B* **85**, 104206 (2012).
- <sup>38</sup>J. K. Krüger, J. Schreiber, R. Jimenez, K.-P. Bohn, F. Smutny, M. Kubat, J. Petzelt, J. Hrabovska-Bradshaw, S. Kamba, and J. F. Legrand, *J. Phys.: Condens. Matter* **6**, 6947 (1994).
- <sup>39</sup>W. A. Phillips, ed., *Amorphous Solids: Low Temperature Properties* (Springer, Berlin, 1981).
- <sup>40</sup>M. A. Ramos, S. Vieira, F. J. Bermejo, J. Dawidowski, H. E. Fischer, H. Schober, M. A. González, C. K. Loong, and D. L. Price, *Phys. Rev. Lett.* **78**, 82 (1997).
- <sup>41</sup>A. I. Krivchikov, A. N. Yushchenko, V. G. Manzhelii, O. A. Korolyuk, F. J. Bermejo, R. Fernández-Perea, C. Cabrillo, and M. A. González, *Phys. Rev. B* **74**, 060201(R) (2006).
- <sup>42</sup>V. A. Konstantinov, A. I. Krivchikov, O. A. Korolyuk, V. P. Revyakin, V. V. Sagan, G. A. Vdovichenko, and A. V. Zvonaryova, *Physica B: Condens. Matter* **424**, 54 (2013).
- <sup>43</sup>R. C. Zeller and R. O. Pohl, *Phys. Rev. B* **4**, 2029 (1971).
- <sup>44</sup>U. Buchenau, Yu. M. Galperin, V. L. Gurevich, D. A. Parshin, M. A. Ramos, and H. R. Schober, *Phys. Rev. B* **46**, 2798 (1992).
- <sup>45</sup>M. A. Ramos and U. Buchenau, *Phys. Rev. B* **55**, 5749 (1997).
- <sup>46</sup>M. A. Ramos and U. Buchenau, *Tunneling Systems in Amorphous and Crystalline Solids*, edited by P. Esquinazi (Springer, Berlin, 1998) p. 527.
- <sup>47</sup>E. Bonjour, R. Calemczuk, R. Lagnier, and B. Salce, *J. Phys. (Paris)* **42**, 63 (1981).
- <sup>48</sup>D. A. Parshin, *Phys. Rev. B* **49**, 9400 (1994).
- <sup>49</sup>M. A. Ramos, *Philos. Mag.* **84**, 1313 (2004).
- <sup>50</sup>J. K. Krüger, J. Baller, T. Britz, A. le Coutre, R. Peter, R. Bactavatchalou, and J. Schreiber, *Phys. Rev. B* **66**, 012206 (2002).
- <sup>51</sup>J. J. Freeman and A. C. Anderson, *Phys. Rev. B* **34**, 5684 (1986).
- <sup>52</sup>A. I. Krivchikov, O. A. Korolyuk, and I. V. Sharapova, *Low Temp. Phys.* **38**, 74 (2012), and references therein.
- <sup>53</sup>J. L. Feldman, M. D. Kluge, P. B. Allen, and F. Wooten, *Phys. Rev. B* **48**, 12589 (1993).
- <sup>54</sup>A. I. Krivchikov, I. V. Sharapova, O. A. Korolyuk, O. O. Romantsova, and F. J. Bermejo, *Low Temp. Phys.* **35**, 891 (2009).
- <sup>55</sup>O. A. Korolyuk, *Low Temp. Phys.* **37**, 416 (2011).
- <sup>56</sup>C. Talón, F. J. Bermejo, C. Cabrillo, G. J. Cuello, M. A. González, J. W. Richardson, A. Criado, M. A. Ramos, S. Vieira, F. L. Cumberera, and L. M. González, *Phys. Rev. Lett.* **88**, 115506 (2002).
- <sup>57</sup>C. Talón, M. A. Ramos, S. Vieira, I. M. Shmyt'ko, N. Afonikova, A. Criado, G. Madariaga, and F. J. Bermejo, *J. Non-cryst. Solids* **287**, 226 (2001).
- <sup>58</sup>M. A. Ramos, M. Hassaine, B. Kabtoul, R. J. Jiménez-Riobóo, I. M. Shmyt'ko, A. I. Krivchikov, I. V. Sharapova, and O. A. Korolyuk, *Low Temp. Phys.* **39**, 468 (2013).
- <sup>59</sup>R. Böhmer, C. Gainaru, and R. Richert, *Phys. Rep.* **545**, 125 (2014).